

Can Thermal Barrier Coatings be Sealed by Metal-Organic Chemical Vapour Deposition of Silica and Alumina?

V.A.C. Haanappel, J.B.A. Scharenborg, H.D. van Corbach, T. Fransen and P.J. Gellings

*University of Twente, Department of Chemical Technology,
P.O. Box 217, 7500 AE Enschede, The Netherlands*

ABSTRACT

Thin Al_2O_3 and SiO_2 films were deposited on thermal barrier coatings (TBC) by means of metal-organic chemical vapour deposition (MOCVD). The thermal barrier coatings consist of ZrO_2 , partially stabilised by MgO (Magnesium Zirconate Amdry 333) and a bond coat of NiAl (Amdry 956). Alumina films were deposited at low temperatures by low pressure MOCVD, carried out in nitrogen gas using aluminium-tri-sec-butoxide (ATSB) as the precursor. Silica films were deposited on the thermal barrier coatings by atmospheric pressure MOCVD with di-acetoxy-di-t-butoxy-silane (DADBS) as the precursor. Besides the deposition of thin oxide films on TBC, pre-oxidation experiments were performed at 600, 800 and 1000°C for 175 h. In order to evaluate the effectiveness of sealing and pre-oxidation, sulphidation experiments were carried out at 600°C for 200 h.

Low pressure deposited alumina films did not show any increased "protective power". Pre-oxidation of the TBC to form a dense and continuous alumina layer on the top of the bond coat also did not show any significant improvement of the protection against sulphide containing gases.

KEY WORDS

thermal barrier coatings (TBC), MOCVD- Al_2O_3 , MOCVD- SiO_2 , sealing, pre-oxidation, sulphidation, plasma-spraying.

1. INTRODUCTION

High reactor temperatures provide higher yields, better selectivity and less hazardous by-products in the process industry. However, at these high temperatures most materials corrode very rapidly in atmospheres containing e.g. O_2 , H_2O , H_2S , SO_2 , CO , CO_2 , CH_4 , HCl and Cl_2 , or in liquids, like molten salts. This results in a short lifetime and high costs /1/.

To avoid corrosion, special coatings have been developed, such as metallic and ceramic coatings. Metallic coatings show a good fatigue and creep resistance and the thermal expansion coefficient is compatible with that of the substrate. However, they have a low chemical resistance against oxidation, sulphidation and carbonation and are therefore not really suitable for protection against high temperature corrosion. Ceramic coatings show a strong chemical

resistance against oxidation, sulphidation and carburisation. Ceramic coatings like Al_2O_3 may become very important for high temperature corrosion protection, but much research has to be performed owing to their brittleness [2].

The use of thermal barrier coatings offers an attractive approach to increase the turbine engine efficiency by increasing the gas inlet temperatures [3,4] and improving the durability/lifetime of the hot components. The increase of the operating temperatures led to the development of materials with a high resistance against high temperature corrosion and improved mechanical properties. Due to the introduction of the thermal barrier coatings with low thermal conductivity, there are now several ways to take advantage of these coatings: 1) the gas inlet temperature may be increased, 2) component cooling at constant gas and metal temperatures may be reduced, and 3) maintaining the gas temperature, the metal temperature may be reduced.

There are two major application techniques to deposit thermal barrier coatings: 1) plasma spraying, and 2) electron-beam, physical vapour deposition. The first is the one mostly used. Zirconia-based coatings have attracted the most attention because of their low conductivity and their relatively high thermal expansion coefficient. In order to stabilise the structure of the zirconia coating, several dopants can be added, for example, yttria, magnesia, and ceria [3]. The degree of stabilisation depends on the amount and composition of the additives [3-5]. In the case of a plasma-sprayed zirconia coating a polymorphic structure is obtained. The high-temperature cubic phase can partially be stabilised by the addition of magnesia.

The most important laboratory experiments on thermal barrier coatings imply thermal expansion, thermal conductivity, thermal cycling behaviour, cyclic oxidation behaviour, hot corrosion behaviour and erosion behaviour.

In this study the protectivity against high temperature corrosion of magnesia stabilised zirconia thermal barrier coatings, sealed by small amounts of silica and alumina deposited by metal organic chemical vapour deposition at atmospheric and low pressure, was examined. The corrosion experiments were performed in a hydrogen sulphide containing gas for 200 h at 600°C.

2. THEORETICAL ANALYSIS

In this part of the paper, a simple mathematical model is presented. In this model, some consequences of changing process parameters are discussed in relation to the penetration depth of the reactants. Notwithstanding the simplicity of this model, it may explain the behaviour and probably predicts the effect of changing parameters on the deposition of thin alumina films. From this point of view, the process parameters can be varied more systematically to obtain the well-desired deposition regime in order to produce a well-adhered and -penetrated oxide film.

In this theoretical approach, where a simple stagnant film diffusion model is presented, the thermal barrier coatings (TBC) are considered as a ceramic matrix with a porous structure. A certain porosity of the coating is necessary in order to reduce local stress, as a consequence of the thermal expansion mismatch between the metallic substrate and the ceramic coating. The pores in the TBC are considered as isothermal cylindrical cavities. The gas is assumed to be stagnant in the pore of infinite length. Other assumptions are that no homogeneous reactions take place inside the pore, no pressure gradient exists along the pore, and the surface reaction of the deposition of alumina from aluminium-tri-sec-butoxide is first order. The concentration of the reactant at the entrance of the pores is determined by the mass transfer through a stagnant film of thickness δ near the interface. If no homogeneous reactions take place, the mass balance of the reactant c in the steady state is given by:

$$-D_{c,\text{eff}} \frac{\partial c}{\partial y} \Big|_y + D_{c,\text{eff}} \frac{\partial c}{\partial y} \Big|_{y+\delta} = 0 \quad (1)$$

where:

$D_{c,\text{eff}}$ = molecular effective diffusion coefficient of reactant c (m^2/s)

y = coordinate perpendicular to the gas/coating interface (m)

The boundary conditions are: $c = c_{\text{bulk}}$ for $y = 0$
 $c = c_{\text{surf}}$ for $y = \delta$

In this case, c_{surf} is the concentration in the direct vicinity of the surface. The mass flux of the reactive compounds c through the film is given by:

$$J_c = \frac{D_{c,eff}}{\delta} (c_{bulk} - c_{surf}) \quad \text{with} \quad \left[\frac{D_{c,eff}}{\delta} \right] = k_s \quad (2)$$

where:

J_c = flux of reactant c through the boundary layer (mol/m².s)

δ = thickness of the diffusion layer (m)

k_g = mass transfer coefficient of reactant c in the gas phase (m/s).

Using the Laplace operator for cylindrical coordinates, the mass balance under steady-state conditions in the pores is given by:

$$D_{c,eff} \left[\frac{\delta^2 c}{\delta r^2} + \frac{1}{r} \frac{\delta c}{\delta r} + \frac{\delta^2 c}{\delta x^2} \right] = 0 \quad (3)$$

where r represents the radial distance, x the axial distance from the entrance of the pore. The effective diffusion coefficient D_{eff} is a function of the tortuosity factor τ (correction factor for the shape of the pores), the molecular diffusion coefficient $D_{c,gas}$ for reactant c in the gas phase, and the Knudsen diffusion coefficient $D_{c,knudsen}$, as follows:

$$\frac{1}{D_{c,eff}} = \tau \left[\frac{1}{D_{c,gas}} + \frac{1}{D_{c,knudsen}} \right] \quad (4)$$

The boundary conditions for a pore of infinite length are:

- on the axis, the radial flux of the reactants is zero, as follows:

$$\left[\frac{\delta c}{\delta r} \right]_{(r=0, x)} = 0 \quad (5)$$

- at the entrance of the pore, the concentration is constant and equal to c_{surf} (arbitrary value):

$$c(r, x=0) = c_{surf} \quad (6)$$

- on the pore wall, the flux of the reactant is proportional to the surface reaction:

$$\left[\frac{\delta c}{\delta r} \right]_{(r=R, x)} = - \frac{k_s c(r=R, x)}{D_{c,eff}} \quad (7)$$

where k_s is the first order rate constant of the surface reaction and R the pore radius.

- For $x \rightarrow \infty$, the concentration of the reactant is zero:

$$c(r, x \rightarrow \infty) = 0 \quad (8)$$

The distribution of the reactant concentration c as a function of the axial and radial position is given by the general solution of the Laplace equation, as follows:

$$\frac{c}{c_{surf}} = 2 \sum_{i=1}^{\infty} \frac{J_0\left(\frac{\alpha_i r}{R}\right) \exp\left(-\frac{\alpha_i x}{R}\right)}{\alpha_i (1 + \delta^2 \alpha_i^2) J_1(\alpha_i)} \quad (9)$$

where J_0 and J_1 are Bessel functions of the first kind, α_i is the roots of the functions J_0 and J_1 , and $\delta = D/(k_s R)$. At the center of the pore, where $r = 0$, the equation can be written as:

$$\left[\frac{c}{c_{surf}} \right]_{(r=0)} = 2 \sum_{i=1}^{\infty} \frac{\exp\left(-\frac{\alpha_i x}{R}\right)}{\alpha_i (1 + \delta^2 \alpha_i^2) J_1(\alpha_i)} \quad (10)$$

If $L \gg R$, equation (10) can be simplified, as follows:

$$\left[\frac{c}{c_{surf}} \right]_{(r=0)} = \frac{2\delta}{(1 + 2\delta)} \exp - \left[\frac{\left(\frac{2}{\delta}\right)^{1/2} x}{R} \right] \quad (11)$$

From equation (11) the distribution of the reactant concentration at position $r = 0$ can be calculated. The effect of the diffusion coefficient, the concentration of the reactant at the entrance of the pore, the surface reaction rate constant, and the pore diameter, on the concentration of the reactant ($c_{(r=0, x)}$) at the axial position x can be determined.

The concentration profile in the pore is now calculated semi-quantitatively from estimated and experimental data. The standard conditions used in this model are given in Table 1. The underlined values are the standard values for calculating the effect of changing the other parameters. The effect of changing the reaction rate constant, interdiffusion coefficient, and pore radius on the distribution of the relative reactant concentration (c/c_{surf}) _{$r=0$} , are shown in Figs. 1-3.

Fig. 1 shows the relative concentration at the axial position x inside the pore as a function of the heterogeneous reaction rate constant. This figure

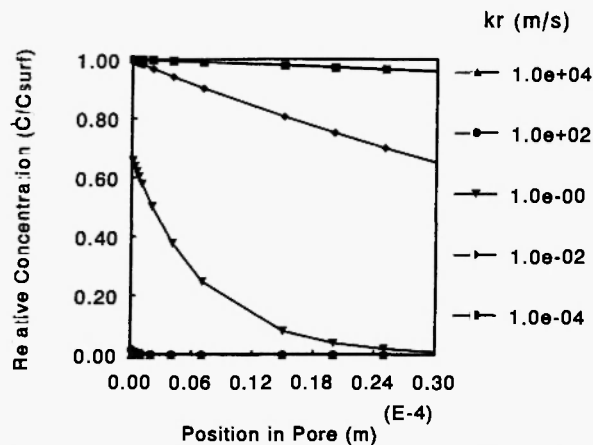


Fig. 1: Relative concentration as a function of the heterogeneous reaction rate constant and the axial position x in the pore.

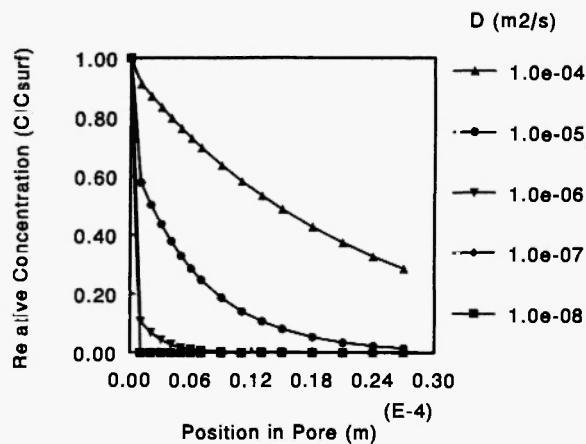


Fig. 2: Relative concentration as a function of the diffusion coefficient and the axial position x in the pore.

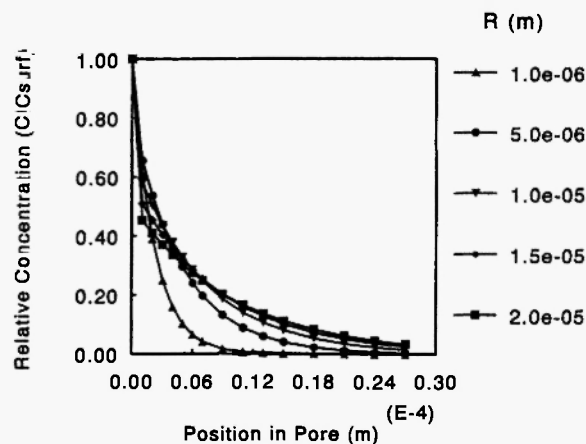


Fig. 3: Relative concentration as a function of the pore radius R and the axial position x in the pore.

Table 1

Parameters used for calculating the concentration profile inside pores

Reaction Rate Constant (k_r , m/s)	Interdiffusion Coefficient (D , m^2/s)	Pore Radius (R , m)
1.10^{-4}	1.10^{-4}	1.10^{-6}
1.10^{-2}	1.10^{-5}	5.10^{-6}
1	1.10^{-6}	1.10^{-5}
100	1.10^{-7}	5.10^{-5}
10,000	1.10^{-8}	1.10^{-4}

indicates that with increasing reaction rate, the relative concentration decreases faster with increasing position x . At high k_r -values, the penetration of the reactant into the pores is almost negligible. At low values of k_r , the gradient of the reaction concentration with the axial position is very low.

Fig. 2 shows the effect of changing the diffusion coefficient on the relative concentration. At very low D -values, the effect of k_r dominates and almost no penetration occurs, while at high values of D the penetration of the reactant is more pronounced.

In Fig. 3 the relative concentration at the axial position x is shown as a function of the pore radius R . Large radii do not have any significant effect on the distribution of the relative concentration along the axial position. Radii smaller than $5 \mu m$ affect the distribution of the reactant more strongly. In this case, the smaller the radius, the steeper the gradient of the relative concentration along the axial position x .

In order to obtain a well-adhering coating on a porous and rough substrate it is recommended that the deposition experiments be performed under well-defined circumstances. The relative concentration of the reactant inside the pores should not drop immediately to zero for very low values of x (axial position). Thus a low reaction rate of the inner surface and a high effective diffusion coefficient are necessary to form a significant amount of alumina on the inner pore surface.

Using a given coating/substrate combination, the diffusion coefficient D , and only slightly the heterogeneous reaction rate constant, k_r , can be influenced by

changing process parameters. To change the reaction rate constant, the catalytic activity of the material can be altered by changing the composition of the porous substrate, but generally, when using one substrate composition, only the deposition temperature can be altered, giving:

$$k_r = k_o \left(\frac{E_a}{RT} \right) \quad (12)$$

where k_o is the pre-exponential factor and E_a the activation energy of the heterogeneous reaction, R the gas constant, and T the temperature in Kelvin.

The diffusion coefficient for binary mixtures of gases can be calculated [6] for pressures up to about 10 atm as a function of the temperature and reactor pressure, as follows:

$$D \approx C_m \frac{T^{1.75}}{P} \quad (13)$$

where C_m is a function of the molecular weight, and P is the pressure in atmospheres.

From these equations it is clear that the reaction rate constant is much more dependent on the temperature than the diffusion coefficient. Furthermore, the diffusion coefficient is inversely proportional to the reactor pressure. A reduction of the process temperature and process pressure may thus improve the deposition inside the pores.

3. EXPERIMENTAL PROCEDURES

Specimen Preparation

Air plasma spraying of the thermal barrier coatings was performed on top of a metallic bond coating. A rod of AISI 304 stainless steel was first blasted with Al_2O_3 (Metco F), then the bond layer (NiAl Amdry 956) was applied in one passage, with a thickness of 0.08 mm. The zirconia layer (Magnesium Zirconate Amdry 333) was applied in two passages with a total thickness of 0.2 mm. (The preparation of the TBC was performed by the University of Eindhoven, The Netherlands.)

SiO_2 coatings were produced by the decomposition of di-acetoxy-di-t-butoxy-silane (DADBS). This precursor was heated in a silicon oil bath to 80°C to

saturate a nitrogen gas flow. This gas flow was diluted with another nitrogen gas flow and saturated with water vapour to obtain the desired gas-phase concentration. The gas was led into a vertical furnace where the specimens were mounted. The total gas stream was 48 l.h⁻¹. The substrate temperature was 560°C, whereas the carrier gas flow and the diluent gas flow were both 24 l.h⁻¹.

The Al_2O_3 coatings were deposited by pyrolysis of aluminium-tri-sec-butoxide (ATSB) in a low pressure chemical vapour deposition (LPCVD) system. It consisted of a horizontal quartz tube reactor (134 cm long, 10 cm in diameter) in a three-zone furnace (Tempress model Omega Junior). A stream of pure nitrogen gas (Praxair nitrogen 5.0) passed through the ATSB precursor in a silicon oil bath. The ATSB had a vapour pressure of 0.133 kPa (1 torr) at 138°C. This saturated gas was diluted with pure nitrogen gas before entering the reactor. The gas line between the ATSB container and the reactor was heated to 150°C to prevent condensation of the precursor. All gas streams were controlled by electronic mass flow controllers (Brooks 5850TR). The linear gas velocity in the reactor was 2.6 m/s. The deposition temperature was monitored by 3 thermocouples which extended into the reactor below the specimens. The temperature profile was maintained as constant as possible ($\pm 0.5^\circ C$) over the length of the specimen load. The reactor pressure during deposition was monitored by capacitive pressure sensors (MKS Baratron type 122A) and kept at the desired value by adding an excess flow of nitrogen to the vacuum pump (Leybold D65BCS). Standard conditions were: deposition temperature: 280°C, partial pressure of ATSB: $9.3 \cdot 10^{-4}$ kPa (ATSB saturation temperature: 138°C), reactor pressure: 0.17 kPa. Pre-oxidation of the thermal barrier coatings was performed in air at 600, 800 and 1000 °C for 175 h.

Tests

The corrosion experiments were carried out at 600°C for 200 h in a closed system. Before starting the experiment, the system was flushed with argon (saturated with water at 15°C) for 20 h with a flow rate of 7 l.h⁻¹ (STP). The mixture of gases (1% H_2S , 1% H_2O , 19% H_2 , bal. Ar.) was introduced afterwards,

with a flow rate of 16 l.h^{-1} . After 2 h the furnace was heated to the desired temperature. The whole system was flushed for another 2 h and then closed. No relevant difference in corrosion rate and corrosion products was obtained between a closed system and a system with a continuous flow, if the reactive gas consumption did not exceed more than 20%.

The morphology and the composition of the layers were investigated by means of optical microscopy and scanning electron microscopy (JEOL M35 CF) equipped with an EDX analysis system (Kevex Delta - class III).

4. RESULTS

Pre-Oxidation

Pre-treatment in air of the coating-substrate systems was performed at three different temperatures. Scanning and optical microscopy revealed that after 175 h exposure at 600 and 800°C the coating showed a good adherence to the NiAl-bond coat. Only for the specimens tested for 175 h at 1000°C the top coat was spalled visibly from the bond coat. Fig. 4a shows a SEM-picture of a cross-section of a thermal barrier coating, annealed for 175 h at 600°C. Fig. 4b shows a partially delaminated thermal barrier coating after 175 h at 1000°C. No difference in the pre-oxidation behaviour was observed between uncoated and SiO_2 or Al_2O_3 -coated specimens.

MOCVD of SiO_2 and Al_2O_3

From the cross sections of SiO_2 -treated thermal barrier coatings, it was clear that under optimum conditions [7] at atmospheric pressure, the deposited oxide layer was only present at the outer surface of the coating. SEM- and EDX-analyses showed that Al_2O_3 coatings deposited at a total pressure of 0.167 kPa, and at a lower deposition temperature of 250°C, showed no significant improvement of the penetration of this oxide into the pores and microcracks of the thermal barrier coatings.

Sulphidation of (Pre-Treated) Specimens

SEM- and EDX-analyses revealed that for all the specimens, as-received, pre-oxidised or coated with an externally applied MOCVD-oxide film, localised corrosion products, in this case NiS, were formed on the outer surface of the specimen. Cross sections of the specimens revealed that after 200 h at 600°C localised radial cracks were formed through the zirconia/magnesia top coat, starting from the bond coat to the outer surface. No significant improvement was obtained after the Al_2O_3 -deposition at reduced pressure, even when the deposition temperature was as low as 220 or 250°C. Next to the formation of cracks in the top coat, also de-adhesion between the bond coat and the top coat was observed. Figs. 5a-d show the cross sections (SEM-pictures) of the specimens treated by different processes.

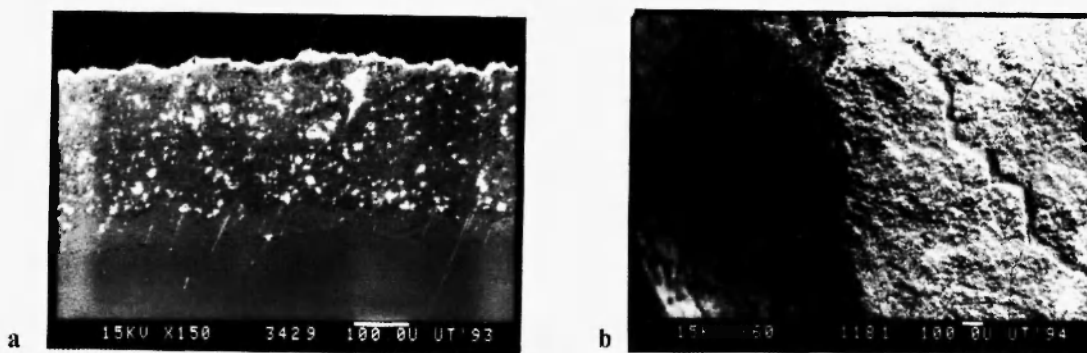


Fig. 4: Cross section (a) of a thermal barrier coating (SEM-image), annealed for 175 h at 600°C, and a partially delaminated thermal barrier coating (b) after 175 h at 1000°C.

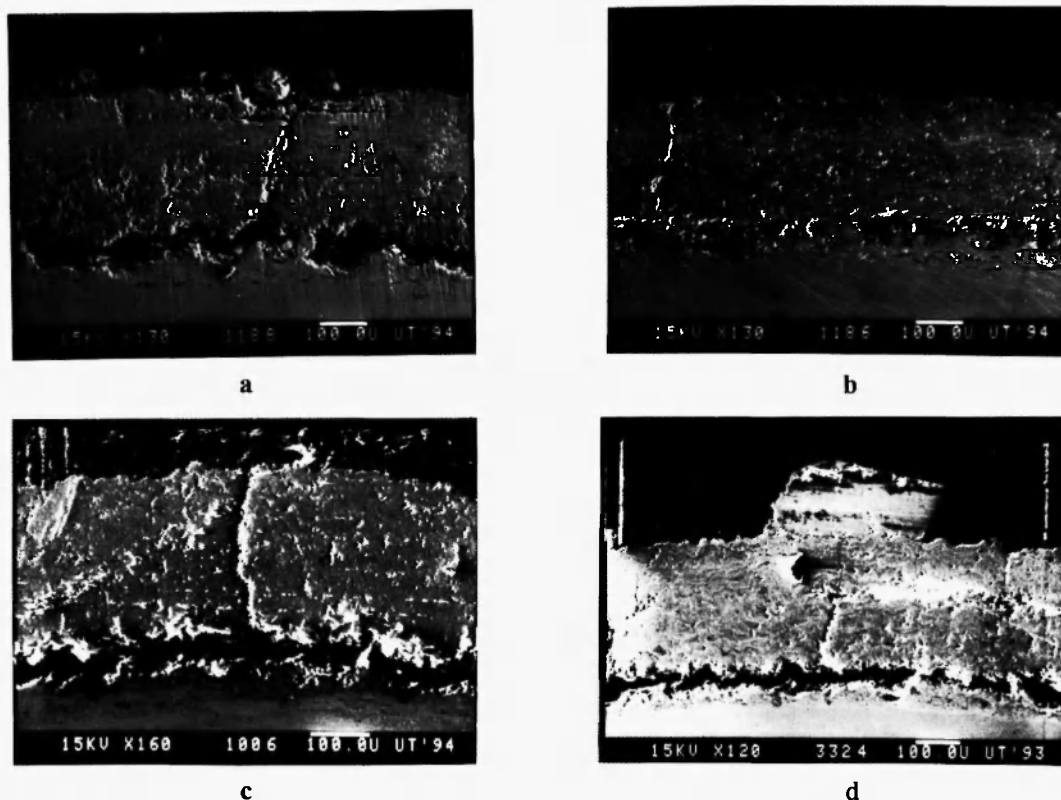


Fig. 5: SEM images of cross sections of specimens tested under sulphidising circumstances, a) no pre-treatment, b) coated with alumina, deposition time: 16 h, deposition temperature: 250°C, c) pre-oxidised for 175 h at 600°C, and d) coated with silica, deposition time: 1 h, deposition temperature: 560°C.

5. DISCUSSION

Pre-treatment in air of the thermal barrier coatings results in the oxidation of the NiAl-bond coat forming outward-grown NiO and NiAl₂O₄-spinel /8,9/. Grabke *et al.* /10/ reported that oxidation of NiAl at high temperatures favours the formation of a protective Al₂O₃-layer. From these observations, it was suggested that an alumina film on the outer side of the bond coat may give the specimen a good protection against high temperature corrosion. The reaction between aggressive compounds such as H₂S and the bond coat might be stopped or reduced significantly. From the results it was clear that after oxidation at temperatures up to 800°C, no de-adhesion of the top coat occurred. Only at 1000°C spallation was observed, which can be explained by the formation of a large compressive stress

in the top coat during oxidation. This means that pre-oxidation can only be carried out at temperatures not much higher than 800°C. From the sulphidation experiments, it was found that this treatment did not improve the protection against high temperature corrosion. The cross-sections showed that the top coat was cracked radially and delaminated from the underlying bond coat after sulphidation. This means that the formation of an internal oxide scale near the interface between the bond and the top coat did not give any significant improvement of the corrosion resistance. Thus, no protective and continuous alumina scales were formed during the pre-oxidising treatment in air at high temperatures.

Spallation of the top coat after a pre-treatment at 1000°C can be explained by 1) a large mismatch between the coefficients of thermal expansion of the

oxide scale and the bond coat, which might induce thermal stress by cooling and by thickening of the oxide scale formed during oxidation at high temperatures, and 2) degradation due to an outward growing oxide, penetrating into pores and microcracks of the top coat, resulting in an increased compressive stress in the top coat. In Fig. 6 a schematic representation is given of the top-coat spalling and buckling mechanism /8,9/. On cooling, the top coat segments are constrained by the pegging effects of the penetrated oxides into microcracks, and as a result a compressive stress will initiate spalling and buckling of the ceramic top coat. This mechanism can also explain the degradation mechanism during exposure in sulphide containing gases at high temperatures. The aggressive reactants, in this case hydrogen sulphide or sulphur, can easily reach the formed oxide, due to the presence of microcracks and pores in the top coat. From the partial pressures of oxygen and sulphur it is calculated that NiS is theoretically the most stable phase. During the sulphidation experiments, the oxides will react with the sulphur to form metal sulphides. Due to a high sulphidation rate, as a result of a highly defective structure, also here the NiS will protrude into the existing microcracks and pores of the top coat. The increasing compressive stress, developed mostly in the top coat, will induce spalling of these. This means that the same mechanism is responsible for degradation of the TBC during sulphidation as described under oxidising circumstances.

Summarising, pre-treatment of TBC in air at high temperatures did not result in any improvement of the corrosion resistance, especially in hydrogen sulphide bearing gases.

Other possibilities to improve the corrosion protection of thermal barrier coatings are 1) preferential oxidation of the bond coat at low partial pressures of oxygen which may result in a protective and continuous alumina layer acting as a diffusion barrier, 2) the formation of a continuous alumina layer by the deposition of an Al_2O_3 -layer by means of CVD. This alumina layer can be applied between the bond and the top coat /8/, 3) doping the NiAl-matrix with yttrium. Grabke *et al.* /10/ reported that high Al-content intermetallics favour alumina formation, but the problem is the sensitivity to spalling of the scale, especially as a consequence of thermal cycling. A high Al content causes a very brittle system. This means that the TBC system with NiAl as a bond coat will degrade very rapidly during exposure in oxidising atmospheres at high temperatures, especially upon thermal cycling. Yttrium, niobium /10/ or hafnium /11/ might suppress oxide spalling, and thus increase the lifetime of the specimen /12/, 4) increasing the TBC-lifetime by pre-oxidation of the bond coat before applying the top coat. Li *et al.* /13/ found that the number of cycles at failure significantly increased after a post spray thermal treatment, and 5) pre-aluminising the bond coat /14,15/.

In addition to the above-mentioned possibilities of increasing the protectiveness of the TBC against high

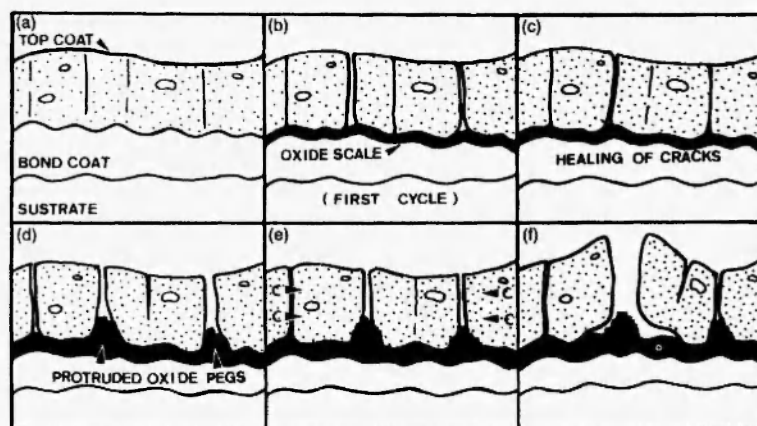


Fig. 6: Schematic representation of the degradation mechanism of thermal barrier coatings during high temperature oxidation /9/.

temperature corrosion, the MOCVD process to deposit dense and continuous thin oxide layers on the outer surface of the top coat may also beneficially affect the corrosion resistance of the TBC. This oxide layer may act as a diffusion barrier against aggressive compounds. These layers were deposited on the outer surface of the top coat. It is well known that thin silica and alumina layers, deposited by means of MOCVD, may show rather good protective properties against high temperature corrosion [7,16-19].

Sulphidation experiments, as described above, revealed that silica deposited at atmospheric pressure did not show any improvement of the corrosion resistance. The silica was found only at the outer surface of the top coat. In order to obtain a better protective oxide film, alumina was subsequently chosen as the oxide film. The reactor pressure and deposition temperature of the MOCVD-process were reduced to produce thin oxide films partly penetrating into the pores of the top coat resulting in a better adherence by mechanical bonding. Reducing the reactor pressure increases the diffusion coefficient of the reactant molecules, as already discussed in the "theoretical analysis". The effect of changing the diffusion coefficient on the penetration depth is given in Fig. 2. Only for very small diffusion coefficients, the reaction rate constant dominates and no penetration is expected. In this case, a change of the diffusion coefficient does not result in a significant improvement of the penetration depth. Only at higher values of the diffusion coefficient, a change of the D-value affects the penetration depth. Therefore, it is recommended to use a reactor pressure as low as possible. In our case the reactor pressure was 1.25 torr.

Sulphidation experiments revealed that the alumina films deposited by low pressure MOCVD also did not give any improvement of the sulphidation resistance. This might be explained by the fact that the driving force to penetrate, in this case the concentration gradient of the metal-organic chemical vapour deposition process, is not high enough. Sealing of the top coat might then be obtained by chemical vapour infiltration, but the low pressure MOCVD did not result in the desired properties, probably due to too small penetration depths of the alumina.

From the results it is clear that neither pre-treatments, pre-oxidation nor thin film deposition by

MOCVD on the outer surface, resulted in any significant improvement of the protectiveness against aggressive gas compounds. Pre-oxidation results in an oxide layer which is sensitive to spalling as a result of thermal cycling, whereas MOCVD, even at reduced pressure and low deposition temperature, did not result in the desired level of sealing of pores and microcracks in the top coat of the TBC system.

6. CONCLUSIONS

- Pre-oxidation during 175 h at 1000°C results in spalling and delamination of the top coat, due to 1) the formation of a high compressive stress in the top coat with increasing oxide thickness, and 2) thermal mismatch between the bond coat and the oxide.
- Pre-treatment in air at 600 and 800°C and silica and/or alumina deposition by means of MOCVD did not give any satisfactory improvement of the corrosion resistance against aggressive compounds.
- MOCVD of silica and alumina layers results only in the deposition of a thin oxide layer on the outer surface of the top coat. No penetration or infiltration of the oxide into the existing microcracks and pores to improve the protectiveness against high temperature corrosion was observed.

ACKNOWLEDGEMENTS

This research was supported by the Innovative Research Programme on Technical Ceramics (IOP-TK) with the financial aid of the Dutch Ministry of Economic Affairs. Thanks are due to G. van Liempd (University of Eindhoven, The Netherlands) for supplying the thermal barrier coatings.

REFERENCES

1. P. Kofstad, *High Temperature Corrosion*, Elsevier Appl. Sci. Publ., Barking, United Kingdom, 1988.
2. P. Hancock, *Mat. Sci. Eng.*, **88**, 303 (1987).
3. R. Burger and I. Kvernes, in: *Proceedings of*

- High Temperature Alloys for Gas Turbines and Other Applications 1986*, part I, W. Betz, R. Brunetaud, D. Coutsouradis, H. Fischmeister, T.B. Gibbons, I. Kvernes, Y. Lindblom, J.B. Marriot and D.B. Meadowcroft (eds.), Reidel Publishing Company, Dordrecht, The Netherlands, 1986; p. 327.
4. D.J. Wortman, B.A. Nagaraj and E.C. Duderstadt, *Materials Science and Engineering*, **A121**, 433 (1989).
 5. L. Lelait, S. Alphere and C. Diot, *Journal de Physique IV*, Colloque C9, supplement au *Journal de Physique III*, **3**, 645 (1993).
 6. R.H. Perry and D. Green, *Chemical Engineer's Handbook*, McGraw-Hill Book Company, U.S.A., 1984.
 7. R. Hofman, *The Protection of Alloys Against High Temperature Corrosion by SiO₂ Coatings*, PhD Thesis, University of Twente, The Netherlands, 1993.
 8. J.H. Sun, E. Chang, C.H. Chao and M.J. Cheng, *Oxidation of Metals*, **40** (5/6), 465 (1993).
 9. B.C. Wu, E. Chang, C.H. Chao and M.L. Tasi, *J. Mat. Sci.*, **25**, 1112 (1990).
 10. H.J. Grabke, M. Steinhorst and M. Brumm, in: *High Temperature Materials for Power Engineering*, E. Bachelet, R. Brunetaud, D. Coutsouradis, P. Esslinger, J. Ewald, I. Kvernes, Y. Lindblom, D.B. Meadowcroft, V. Regis, R.B. Scarlin, K. Schneider and R. Singer (eds.), Kluwer Academic Publishers, Dordrecht, The Netherlands, 1990.
 11. J. Stringer, I.M. Allam and D.P. Whittle, *Thin Solid Films*, **45**, 377 (1977).
 12. S. Stecura, *Thin Solid Films*, **182**, 121 (1989).
 13. W. Lih, E. Chang, B.C. Wu and C.H. Chao, *Oxidation of Metals*, **36** (3/4), 221 (1991).
 14. B.C. Wu, C.H. Chao, E. Chang and T.C. Chang, *Mater. Sci. Eng.*, **A124**, 215 (1990).
 15. B.C. Wu, E. Chang, D. Tu and S.L. Wang, *Mater. Sci. Eng.*, **A111**, 201 (1989).
 16. V.A.C. Haanappel, *Alumina Films on Metallic Substrates by MOCVD*, PhD Thesis, Enschede, The Netherlands, 1994.
 17. H.D. van Corbach, V.A.C. Haanappel, T. Fransen and P.J. Gellings, *Thin Solid Films*, **239**, 31 (1994).
 18. V.A.C. Haanappel, H.D. van Corbach, T. Fransen and P.J. Gellings, *Surface and Coatings Technology*, **63**, 145 (1994).
 19. V.A.C. Haanappel, H.D. van Corbach, T. Fransen and P.J. Gellings, *Surface and Coatings Technology*, **64**, 183 (1994).